JOURNAL OF NATURAL REMEDIES
DOI: 10.18311/jnr/2025/50286
RESEARCH ARTICLE

Nardostachys jatamansi Mitigates Radiation-induced Depressive Behaviour: Evidence from Behavioural Assessment and Computational Insights into Multi-target Mechanisms

B. Deepa[1], Shyamjith Manikkoth[2], Aswin Mohan[3], Rajesh Raju[3] and Anuroopa G. Nadh[3*]

[1]Department of Pharmacology, KS Hegde Medical Academy (KSHEMA), Nitte (Deemed to be University), Mangalore – 575018, Karnataka, India

[2]Department of Pharmacology, Kanachur Institute of Medical Sciences and Research Centre, Mangalore – 575018, Karnataka, India

[3]CIODS (Centre for Integrative Omics Data Science), Yenepoya (Deemed to be) University, Mangalore – 575018, Karnataka, India; anuroopasanju@gmail.com

Abstract

Background: Radiation-induced depression is a significant neuropsychiatric consequence following therapeutic exposure to ionising radiation. *Nardostachys jatamansi* (*N. jatamansi*), a medicinal herb widely used in Ayurvedic medicine, is well-recognised for its neuroprotective and antidepressant properties. **Aim:** This study aimed to evaluate the antidepressant activity of *N. jatamansi* Ethanolic Extract (NJEE) in a mouse model of electron beam radiation-induced depression and to explore its potential molecular mechanisms against key targets of depression using computational approaches. **Methods:** Mice that were exposed to electron beam radiation were assessed for depressive-like behaviours using the Forced Swim Test (FST) and Tail Suspension Test (TST). NJEE was administered post-radiation, and behavioural outcomes were recorded. To elucidate the molecular basis of its antidepressant effects, molecular docking of 248 phytochemicals from *N. jatamansi* was performed against depression-associated targets: the $GABA_B$ receptor, Monoamine Oxidase A (MAO-A), and Monoamine Oxidase B (MAO-B). Compounds with high docking scores were further analysed using 100 ns molecular dynamics simulations and binding free energy calculations. **Results:** NJEE-treated mice exhibited significantly reduced immobility time in both the FST and TST, indicating notable antidepressant activity. Docking studies revealed that 76, 107, and 111 phytochemicals demonstrated stronger binding affinities toward the $GABA_B$ receptor, MAO-A, and MAO-B, respectively, compared to standard ligands. Remarkably, 73 compounds showed binding interactions with all three targets. Molecular dynamics simulations confirmed the stability of the top ligand-receptor complexes, and binding energy analyses further supported the potential efficacy of these compounds. **Conclusion:** NJEE exhibits significant antidepressant effects in a radiation-induced depression model in mice. *In silico* findings suggest that multiple phytoconstituents in NJEE may modulate key molecular targets implicated in depression, highlighting its potential as a multi-target therapeutic agent for depressive disorders associated with radiation exposure.

Major Findings: NJEE showed protective activity against the radiation-induced depression model in mice. *In silico* analysis revealed that its phytoconstituents could interact with multiple key targets of depression with high affinity, suggesting its potential as a multi-target therapeutic agent.

Keywords: Antidepressant, *In Silico*, *In Vivo*, *Nardostachys jatamansi*, Radiation-induced Depression

1. Introduction

Electron Beam Radiation (EBR) is a type of ionising radiation that carries high-energy electrons capable of penetrating biological tissues and inducing ionisation, which can lead to cellular and DNA damage. Ionising radiation, including EBR, is widely recognised for its ability to cause oxidative stress, disrupt neural circuits,

*Author for correspondence

Article Received on: 05.07.2025 Revised on: 07.08.2025 Accepted on: 20.08.2025

and impair neurotransmitter balance, contributing to the pathogenesis of neuropsychiatric disorders such as depression[1]. Despite these risks, EBR has found significant utility in modern industries and healthcare settings. In healthcare, electron beam therapy is used as a precise form of external beam radiotherapy for treating superficial cancers such as skin cancers, head and neck tumours, and chest wall recurrences of breast cancer[2]. EBR is also applied in the sterilisation of medical devices, pharmaceuticals, and biological products due to its ability to eliminate pathogens without using high temperatures or chemical agents[3]. Additionally, EBR is employed in food processing to reduce microbial load and extend shelf life[4]. Although EBR has therapeutic benefits, its exposure can lead to adverse biological effects, especially in the central nervous system, where oxidative damage and neurotransmitter imbalances can result in conditions such as radiation-induced depression[5]. The management of such complex neuropsychiatric side effects remains a clinical challenge, prompting research into plant-based neuroprotective agents.

Nardostachys jatamansi, a valuable medicinal herb native to the Indian Himalayas, has been traditionally used in Ayurveda and Unani medicine since approximately 800 BC for its broad spectrum of therapeutic properties[6]. The plant's rhizomes and roots have been widely used for their sedative, diuretic, carminative, antispasmodic, hepatoprotective, and neuroprotective effects[7]. *N. jatamansi* has been employed in the treatment of epilepsy, insomnia, cholera, palpitations, convulsive disorders, liver dysfunction, gastrointestinal disturbances, and psychological disorders such as mania[6,8]. It is also used to enhance appetite, relieve flatulence, support digestion, promote hair growth, improve skin complexion, and maintain cardiovascular health[7,9]. Despite its extensive traditional use, the specific molecular mechanisms through which *N. jatamansi* may counteract neuropsychiatric disorders, particularly radiation-induced depression, remain insufficiently elucidated.

This study is a continuation of the previous investigation by the same group of researchers that initially screened the antidepressant activity of NJEE in electron beam radiation (EBR)-induced depression[5]. The present study aimed to investigate the potential antidepressant activity of NJEE in EBR-induced depression using validated mouse models and behavioural assessments in greater detail. Furthermore, advanced *in silico* approaches were utilised to explore the molecular interactions of bioactive phytochemicals from *N. jatamansi* with key neurochemical targets implicated in depression to assess the possible regulatory effect. This integrative experimental and computational approach seeks to provide novel insights into the therapeutic potential of NJEE in managing radiation-induced depressive disorders.

2. Materials and Methods

2.1 Animals

Healthy adult Swiss albino mice of both sexes, 3-6 months of age, weighing 20-25 g, were used after obtaining ethical clearance from the institutional animal ethical committee. They were kept under standard housing conditions, maintained at a room temperature of 25±1 °C, with a 12:12 hour light/dark cycle. They had free access to a standard pellet diet and water orally. Animals were kept in separate cages.

2.2 *Nardostachys jatamansi* Ethanolic Extract

For preparing the ethanolic extract, a weighed quantity (500g) of *N. jatamansi* root powder obtained from Rajesh chemicals, Mumbai, was used and extracted with ethanol (90%) in a Soxhlet apparatus. The extract was concentrated on a rotary evaporator at a temperature not exceeding 60 °C. The dried molten mass was chocolate brown and was stored in a refrigerator. This was then dissolved in distilled water every day for further use. NJEE was administered at a dose of 100mg/kg in this study.

2.3 Radiation

Radiation procedure was done at Microtron Centre, Mangalore University. Animals were restrained in well-ventilated Perspex boxes and exposed to whole body electron beam radiation at a distance of 30 cm from the beam exit point of the Microtron accelerator at a dose rate of 72 Gy/min. Appropriate and required safety measures were taken while handling and housing irradiated animals. Animals were exposed to three different (2 Gy, 4 Gy) doses of EBR.

2.4 Assessment of Depression

Assessment of depression was done by the following tests.

2.4.1 Forced Swimming Test (FST)

The FST is the most widely used pharmacological model for assessing antidepressant activity. The development of immobility when the rodents are placed in an inescapable cylinder of water reflects the cessation of persistent escape-directed behaviour. The apparatus consists of a clear plexiglass cylinder (20 cm high X 12 cm diameter) filled to 15 cm depth with water. This depth was sufficient to keep the mice from supporting themselves by placing their paws or tails on the base of the cylinder. Water was changed between each swim session to prevent possible effects of an alarm substance released by rats during the swim session. During the test session, the immobility time was recorded for 5 minutes, when the mice made no further attempts to escape, and made only movements to keep their heads above the water[5].

2.4.2 Tail Suspension Test (TST)

The TST is the second method for assessing the depressive state. A cord of about 50 cm in length was stretched between two metal tripods at a height of 70 cm, to which the mice were attached by the tail with sticky tape. After the initial period of vigorous motor activity, the mice became still, and the immobility time was measured with a stopwatch for a total duration of 8 minutes. Mice were considered immobile when they hung passively and were completely motionless[5].

2.5. Target Selection and Preparation

The key targets of depression, $GABA_B$ receptor, MAO-A, and MAO-B were selected for the docking study. The X-ray crystallographic structure files of the targets ($GABA_BR$ (PDB ID: 4MS3), MAO-A (PDB ID: 2Z5Y), and MAO-B (PDB ID: 1OJ9), having resolution 2.5 Å, 2.17 Å, and 2.3 Å, respectively) were downloaded from the Protein Data Bank (PDB)[10]. All these three receptors were considered for virtual screening against the selected phytochemicals of *N. jatamansi* using the molecular docking suite, Discovery Studio (DS) client version (Dassault Systems BIOVIA, Discovery Studio Modelling Environment, Release 2020, Dassault Systems: San Diego, CA, USA). Before docking, the target structures were prepared by protonation, loop modelling, and optimisation of side-chain conformations, following the target preparation protocols outlined in DS.

2.6. Phytochemical Selection and Preparation

A comprehensive literature search was conducted using the PubMed database to identify phytochemicals from *N. jatamansi* that had been characterised through various experimental techniques. To compare the affinity and interactions of these residues with the receptors, the endogenous ligand GABA of $GABA_BR$, Clorgyline and Pargyline, the known inhibitors of MAO-A and MAO-B, respectively, were considered as controls for the docking study. The 3D conformers of all these compounds were retrieved from the PubChem (PC) database in SDF format. Before docking, all compounds, including phytochemicals and reference molecules, were prepared using the ligand preparation wizard in DS, which involved duplicate removal and enumeration of isomers and tautomers.

2.7 Molecular Docking

Virtual screening of all three receptors against the selected phytochemicals was performed using the site-feature-based docking algorithm 'LibDock' of DS. LibDock is a rigid-body docking tool which docks ligands by matching their polar and apolar features to hot spots within the protein binding site. Binding sites were defined based on the coordinates of the natural ligand binding pockets. Docking parameters were set with 100 hot spots, a tolerance of 0.25, and 'FAST' mode for conformation generation, allowing up to 255 conformations per ligand; all other settings were kept at default. After docking, the compounds were ranked by LibDock scores, where higher scores indicate more favourable binding modes.

2.8 Molecular Dynamics

Next, to estimate the binding stability, top-ranked compounds were subjected to Molecular Dynamics (MD) simulations using GROMACS 2023[10]. The CHARMM36 force field was applied, and topology files were generated separately for protein and ligand via pdb2gmx and CGenFf server, respectively.

Systems were solvated in a TIP3P water triclinic box and neutralised with monoatomic ions (Na^+ and Cl^-) using genion. Energy minimisation was performed, followed by thermostat coupling. Equilibration was carried out under NVT and NPT ensembles for 200 picoseconds. Production MD was run for 100 nanoseconds, utilising Graphics Processing Unit (GPU) acceleration for nonbonded interactions and Central Processing Unit (CPU) for bonded/ Public Market Equivalent (PME) calculations. The stability of target-ligand complexes was estimated through Root Mean Square Deviation (RMSD) and Root Mean Square Fluctuation (RMSF) trajectory analyses.

2.9 Binding Free Energy Calculations

Binding free energies were estimated to check the binding stability of target-ligand complexes in terms of their energies. The Molecular Mechanics Poisson-Boltzmann Surface Area (MMPBSA) method, which combines molecular mechanics energies with implicit solvation models, was employed to evaluate protein-ligand binding affinities. Calculations were performed using the gmx_MMPBSA tool[11] on MD trajectories. The following equation was used to calculate the binding energy.

$$\Delta G_{bind} = G_{complex} - (G_{receptor} + G_{ligand})$$

Where G corresponds to free energy, ΔGB corresponds to the change in binding free energy.

3. Results

3.1 Forced Swimming Test Assessment Indicates Antidepressant Effect of NJEE in EBR-Induced Depression

The results from the Forced Swimming Test revealed significant findings regarding the antidepressant potential of NJEE in EBR-induced depression. Mice exposed to 2 Gy and 4 Gy of radiation showed a marked increase in immobility time (230.58 ± 4.27 sec and 241.41 ± 3.52 sec, respectively), indicating severe depression-like behaviour compared to the normal control group (137.17 ± 28.74 sec). Pretreatment with NJEE at 100 mg/kg significantly reduced the immobility time in both radiation groups77.83 ± 4.44 sec in the 2 Gy group and 84.33 ± 3.11 sec in the 4 Gy group, suggesting strong antidepressant and neuroprotective effects. Statistical analysis using one-way ANOVA followed by Tukey-Kramer post-hoc test confirmed that these differences were very highly significant ($p < 0.001$). Overall, the findings suggested that NJEE 100 mg/kg effectively ameliorates radiation-induced depression in mice (Table 1).

3.2 Tail Suspension Test Assessment Indicates Antidepressant Effect of NJEE in EBR-Induced Depression

The results from the Tail Suspension Test (TST) demonstrate the significant antidepressant effect of NJEE at 100 mg/kg in mitigating radiation-induced depression in mice. Mice exposed to EBR at 2 Gy and 4 Gy exhibited markedly increased immobility times (219.5 ± 5.23 sec and 238.16 ± 4.61 sec, respectively) compared to the normal control group (163.11 ± 31.95 sec), indicating the induction of depression-like behaviour. However, pre-treatment with NJEE significantly reduced the immobility durations in both radiation-exposed groups-to 102.58 ± 5.98 sec in the 2 Gy group and 112.83 ± 3.81 sec in the 4 Gy group-suggesting a strong antidepressant and neuroprotective effect. Additionally, NJEE alone (100 mg/kg) drastically reduced immobility time (46.08 ± 2.94 s), further supporting its intrinsic antidepressant activity. These findings indicate that NJEE can significantly counteract the depressive behavioural effects of radiation exposure (Table 2).

Table 1. Effect of *Nardostachys jatamansi* ethanol extract on depression using the forced swimming test

	Group	Duration of immobility in seconds
1	Normal (DW)	137.17±28.73
2	NJEE 100mg/kg	46.08 ±2.94[a]
3	2 Gy	230.58 ± 4.27[a]
4	NJEE 100mg/kg +2 Gy	77.83 ± 4.44[b]
5	4 Gy	241.41 ± 3.52[a]
6	NJEE 100mg/kg + 4 Gy	84.33±3.11[b]

*One-way ANOVA followed by Tukey-Kramer test. N=12; NJEE: *Nardostachys jatamansi* ethanolic extract; DW: Distilled Water; a: p<0.001, considered very highly significant compared to the normal group. b: p<0.001, considered very highly significant compared to the respective non-treated radiation group.

3.3 Molecular Docking

A total of 248 phytochemicals were retrieved based on the literature analysis (Table 1). Docking analysis showed that the majority of the phytochemicals bind to the selected targets, $GABA_BR$, MAO-A, and MAO-B, with greater affinity than the controls GABA (PC ID: 119), Clorgyline (PC ID:4380) and Pargyline, respectively (PC ID: 4688). The phytocompounds that exhibited higher docking scores than the controls against the selected targets are represented in their PubChem IDs (Figure 1).

The phytochemicals are depicted by blue outer circles corresponding to their PubChem IDs. The inner circle indicates the respective docking scores, while the central circle represents the selected target with its associated PDB ID.

From the docking analysis, it was observed that the majority of compounds from the medicinal plants mediate a stronger affinity towards all three targets than the controls. Also, it was observed that many of the phytochemicals commonly interact with all three selected key receptors associated with depression (Figure 2).

From the figure, it is evident that the 73 phytochemicals were interacting with all three selected targets in common with great affinity compared to the respective controls. A total of 76, 106, and 110 compounds interacted with higher affinity than the controls against $GABA_BR$, MAO-A, and MAO-B, respectively. Table 3 displays the docking parameters of the top-scoring compounds and controls with their respective targets.

Table 2. Effect of *Nardostachys jatamansi* ethanol extract on depression using the tail suspension test

Group		Duration of immobility in seconds
1	Normal (DW)	163.11 ± 31.95
2	NJEE 100mg/kg	46.08 ±2.94 [a]
3	2 Gy	219.50 ± 5.23 [a]
4	NJEE 100mg/kg +2 Gy	102.58 ± 5.98 [b]
5	4 Gy	238.16 ± 4.61 [a]
6	NJEE 100mg/kg + 4 Gy	112.83±3.81 [b]

One-way ANOVA followed by Tukey-Kramer test. N=12
a: p<0.001, considered very highly significant compared with the normal group; b: p<0.001, considered very highly significant compared with the respective non-treated radiation group.

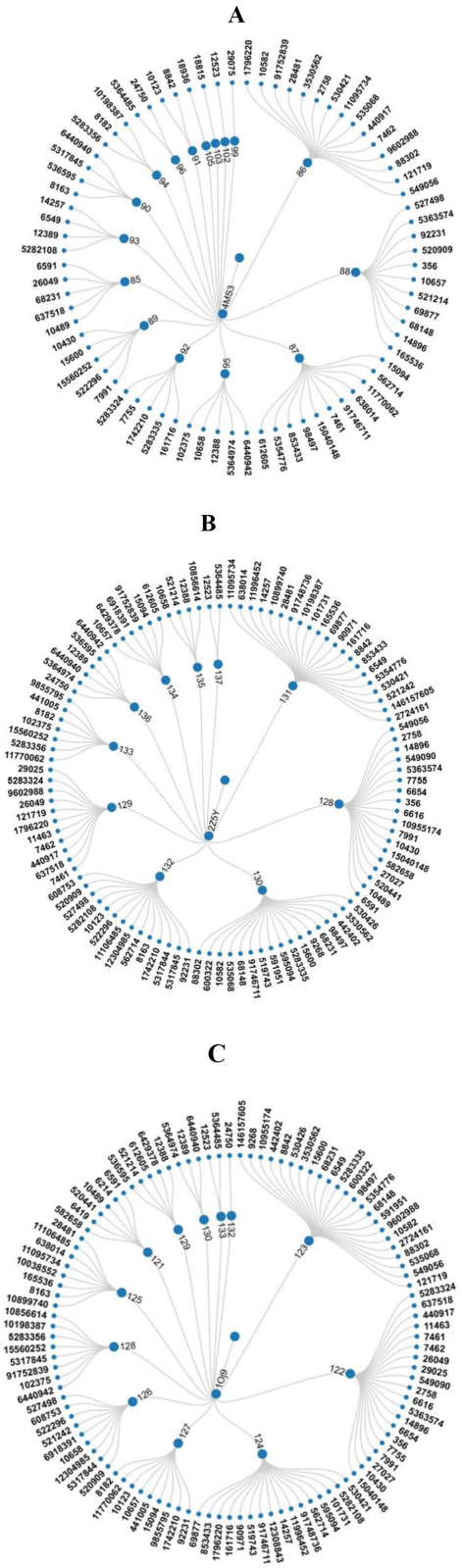


Figure 1. List of phytochemicals of *Nardostachys jatamansi* that exhibited higher docking scores than the controls against the receptors $GABA_BR$ (A), MAO-A (B), and MAO-B (C).

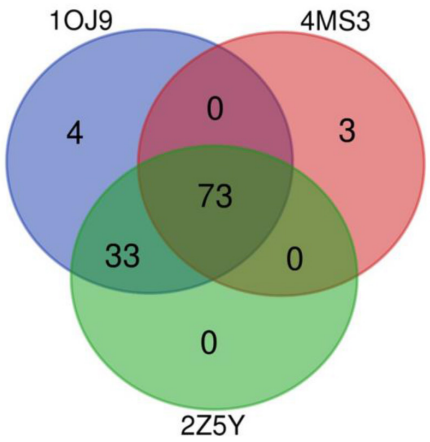
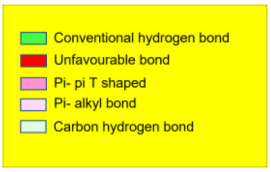


Figure 2. Venn diagram representing the no. of phytochemicals of *Nardostachys jatamansi* interacting with the targets GABABR (PDB ID: 4MS3), MAO-A (PDB ID: 2Z5Y), and MAO-B (PDB ID: 1OJ9).

The binding modes of top-ranked phytochemicals to the respective targets are represented in Figure 3.



3.4 Molecular Dynamics

Molecular dynamics simulations were performed to assess the binding stability of the selected phytochemicals to their respective targets. The results showed that all three target-ligand complexes remained stable throughout the simulation period. The protein backbone deviation (RMSD) and individual amino acid fluctuation (RMSF) results are shown in Figure 4.

Table 3. Docking parameters of top-scoring phytochemicals from *Nardostachys jatamansi* against selected molecular targets associated with depression

Targets	Ligands with PubChem IDs	LibDock Score	Interacting Amino Acids
$GABA_BR$ (PDB ID: 4MS3)	1-Eicosene (18936)	105.00	Trp65, Lys 102, Cys103, Cys129, His170, Trp278, tyr250
	GABA (119, control)	70.44	Trp65, Ser153, His170, Trp278
MAO-A (PDB ID: 2Z5Y)	Phytane (12523)	137.89	Arg51, Val303, Lys305, Phe352, Trp397, Cys406, Tyr407, Ala448
	Clorgyline (4380, control)	118.66	Tyr69, Tyr407, Gly443, Tyr444, Met445
MAO-B (PDB ID: 1OJ9)	Phytane (12523)	133.90	Ile14, Arg42, Tyr60, Phe343, Tyr398, Tyr435, Ala439, Met436
	Pargyline (4688, control)	99.91	Tyr60, Phe343, Tyr435, Met436

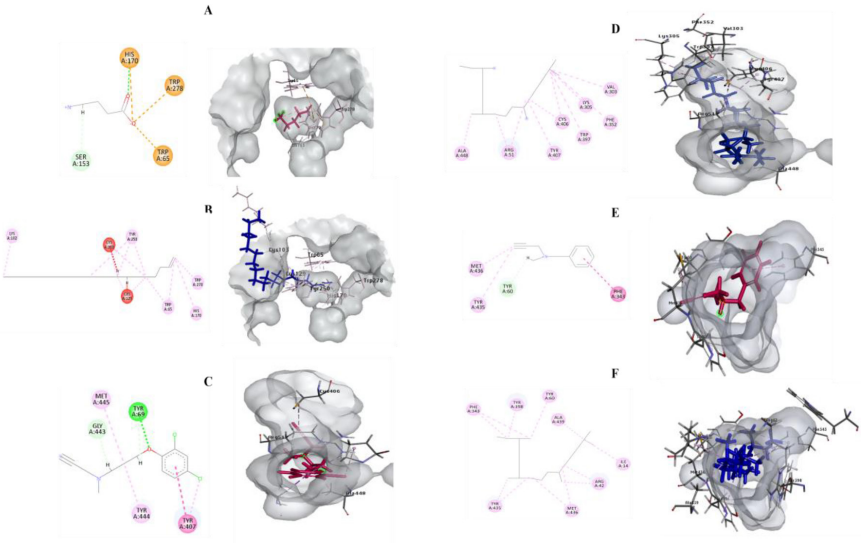


Figure 3. The binding mode of top-ranked phytochemicals of *Nardostachys jatamansi* in the binding pocket of selected key targets of depression as identified through molecular docking studies. The 2D and 3D representations of molecular interactions between target and ligands, alongside the controls, are shown on the Right-Hand Side (RHS) and Left-Hand Side (LHS), respectively. The blue-colored compounds in RHS represent the phytochemicals, while the magenta-colored compounds represent the controls. The figure representation is as follows: **A.** GABABR-GABA (control); **B.** GABABR- 1-Eicosene; **C.** MAO-A-Clorgyline (control); **D.** MAO-A-Phytane; **E.** MAO-B- Pargyline (control); **F.** MAO-B-Phytane. The nature of the interaction is represented as colored lines as follows.

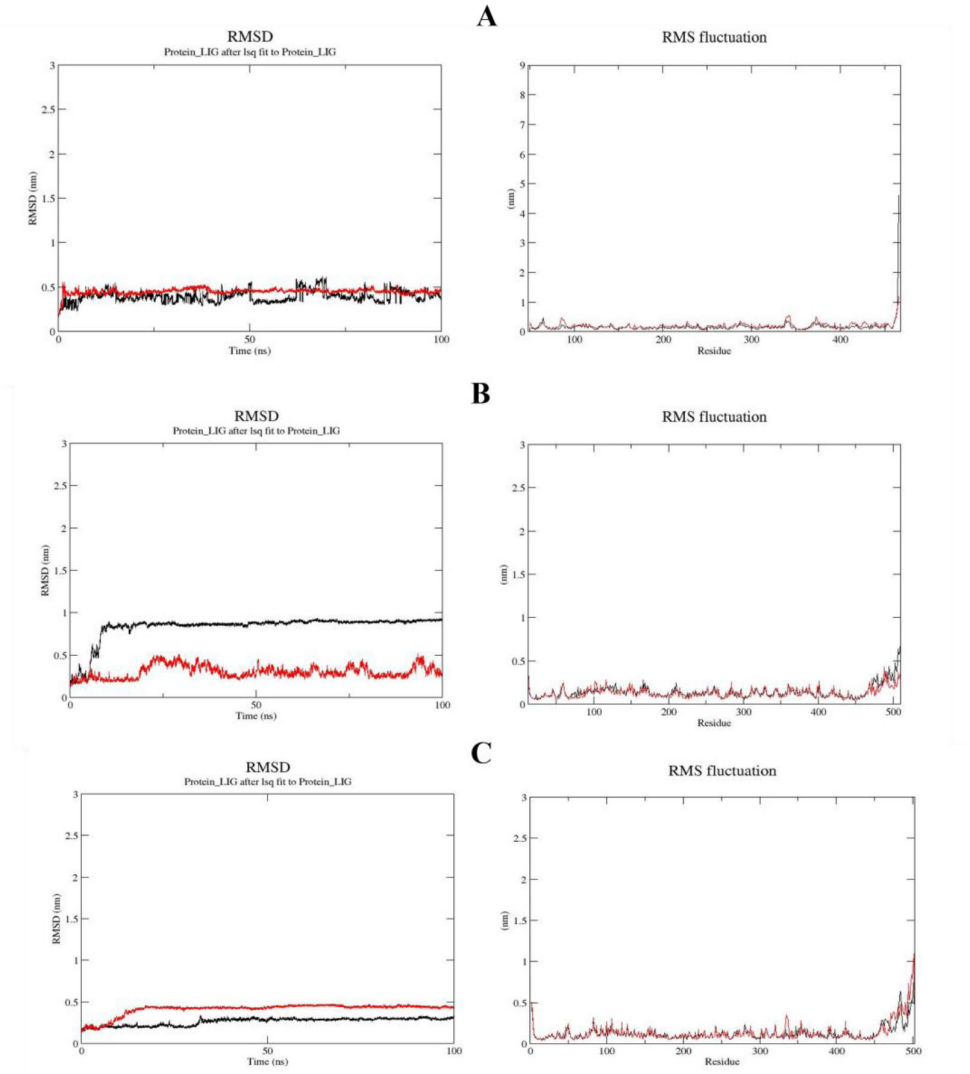


Figure 4. RMSD and RMSF plots over a 100-nanosecond molecular dynamics simulation for selected phytochemicals of *Nardostachys jatamansi* complexed with key targets of depression. The image representation is as follows: **A.** GABABR-GABA (control) and GABABR-1-Eicosene; **B.** MAO-A-Clorgyline (control)and MAO-A- Phytane; **C.** MAO-B- Pargyline(control) and MAO-B-Phytane. The left-hand side represents RMSD, and the right-hand side represents RMSF. The phytochemical-bound receptors are indicated in red colour, where the endogenous ligand and drug (control)-bound structures are represented in black colour.

Table 4. The binding free energy parameters of top top-ranked target-ligand complexes identified from docking studies

Energy Components	1OJ9-12523		2Z5Y-12523		4MS3-18936	
	Binding Energy	Standard Deviation	Binding Energy	Standard Deviation	Binding Energy	Standard Deviation
ΔVDWAALS	-54.55	0.78	-56.55	1.06	-12.08	0.2
ΔEEL	-0.53	1.25	-0.31	0.57	-0.23	1.07
ΔEPB	33.9	0.82	36.08	0.26	4.09	1.02
ΔENPOLAR	-4.86	0.03	-4.82	0.03	-1.8	0.24
ΔGGAS	-55.08	1.75	-56.86	1.48	-12.32	1.5
ΔGSOLV	29.04	0.82	31.26	0.26	2.29	1.05
ΔTOTAL	-26.04	1.94	-25.6	1.5	-10.03	1.83

The binding free energy values of target-ligand complexes are expressed in kcal/mol. Receptors are represented by their PDB IDs, while phytochemicals are represented by their PubChem IDs.

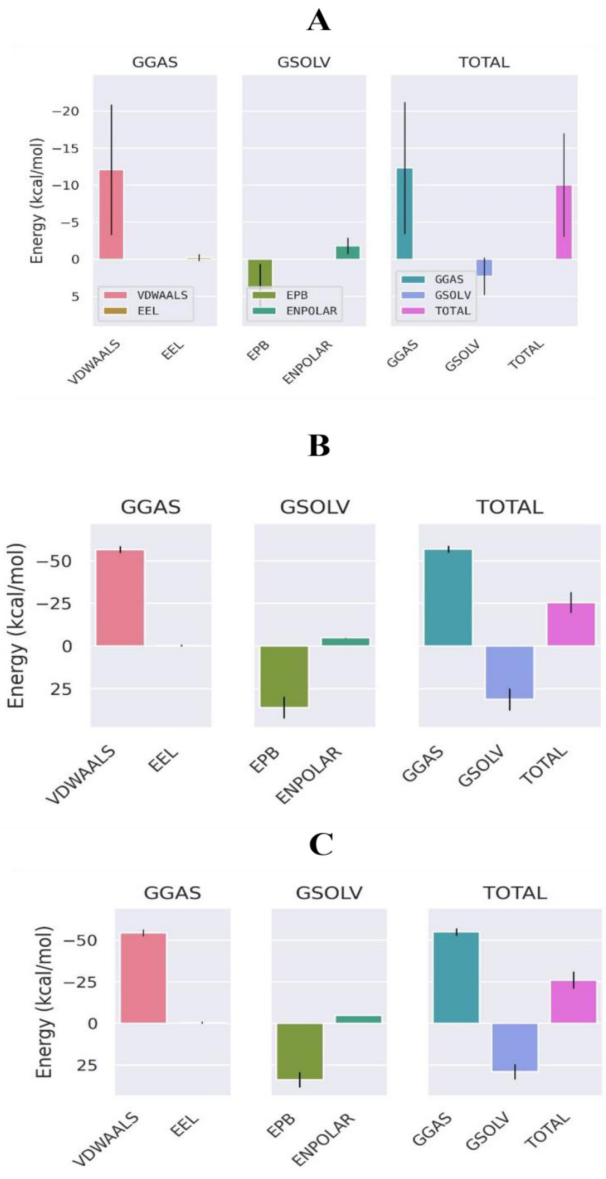


Figure 5. Binding free energy distribution for target-Ligand complexes. The y-axis represents energy in kcal/mol. The X-axis denotes energy contribution phases. The image representation is as follows: A. GABABR-1-Eicosene; 5. MAO-A- Phytane; 5. MAOB-Phytane.

*GGAS-gas phase energies, GSOLV-solvation energies, VDWAALS-van der Waals energy, EEL-electrostatic energy, EPB-electrostatic solvation energy, ENPOLAR-non-polar solvation energy, TOTAL: total binding free energy.

3.5 Binding Free-energy Calculations

After the dynamics, the binding free energies of target-ligand complexes were analysed using MMPBSA to check the binding stability. The parameters of free energy change calculations are listed in Table 4, and the associated energy contributions are represented as a bar chart in Figure 5.

4. Discussion

In this pre-clinical study, pharmacological experiments demonstrated that the ethanolic extract of *N. jatamansi* exhibits significant antidepressant activity against electron beam radiation-induced depression in Swiss albino mice. Animals exposed to electron beam radiation displayed marked depressive-like behaviour, as evidenced by a significant increase in immobility time in both the FST and the TST. Treatment with NJEE effectively reduced immobility time in these behavioural assessments, indicating its potential antidepressant effects.

To analyse the possible molecular mechanism underlying, computational predictive analysis was carried out using different *in silico* tools. Interestingly, molecular docking analysis revealed a notable finding where, out of 248 screened compounds, 73 compounds demonstrated high affinity to all three key targets in common. Among these, 77 compounds showed higher binding affinity toward the $GABA_B$ receptor, 107 compounds exhibited greater affinity for the MAO-A receptor, and 111 compounds showed superior binding to the MAO-B receptor compared to the respective control compounds.

Recently, the involvement of GABA in the pathophysiology of depression has gained considerable attention. GABA, the primary inhibitory neurotransmitter in the central nervous system, may contribute to depressive disorders by acting through the $GABA_B$ receptor[12,13]. Activation of $GABA_B$ receptors has been shown to decrease serotonin release, which is closely associated with mood regulation[14]. This is supported by evidence that $GABA_B$ receptor antagonists exhibit significant antidepressant-like potential in animal models of depression[18]. As a metabotropic receptor for GABA, the $GABA_B$ receptor has emerged as a promising therapeutic target in the development of novel antidepressant agents[12-15]. Small molecules capable of modulating $GABA_B$ receptor function are actively being investigated as potential therapeutic strategies for treating depression[16,17].

From the docking analysis in this study, it was observed that several natural compounds from the medicinal plant *N. jatamansi* exhibited higher binding affinity for the $GABA_B$ receptor compared to the endogenous ligand, GABA. Among the screened

phytochemicals, 1-Eicosene demonstrated the highest docking score of 105, while the control ligand GABA showed a much lower score of 70.01. Experimental studies have identified Trp278 in domain 2 as a critical residue for agonist activity[18]. Consistent with these findings, the docking results from the present study also revealed interactions between Trp278 and both the control ligand GABA and the phytochemical 1-Eicosene (Figures 3A and 3B). Additionally, His170 and Trp65 were common interaction sites for both GABA and 1-Eicosene. Notably, additional interactions were observed for 1-Eicosene with Lys102 and Tyr250, which were absent in GABA binding. These results suggest that the natural compounds not only exhibited a higher docking score but also formed a greater number of stabilising interactions, while adopting a similar orientation in the $GABA_B$ receptor binding cleft as GABA. Collectively, these findings provide indirect but compelling evidence that the selected phytochemical may act as a competitive inhibitor of the $GABA_B$ receptor.

MAO and MBO are mitochondrial enzymes highly expressed in neuronal, gastrointestinal, and hepatic tissues. They play a critical role in the oxidative deamination of monoamine neurotransmitters such as serotonin, norepinephrine, and dopamine, which are central to the regulation of mood and the pathophysiology of depressive disorders[19,20]. By controlling the synaptic levels of these neurotransmitters, MAOs significantly influence mood homeostasis and are directly implicated in the development of anxiety and depression[21]. Consequently, MAO Inhibitors (MAOIs) are clinically utilised to elevate monoamine levels and are effective in the treatment of various Central Nervous System (CNS) disorders, including major depressive disorders[19-22].

From the dynamic simulation, it is evident that both 1-Eicosene-bound and GABA-bound $GABA_BR$ structures show low and stable RMSD values (~0.3–0.4nm) throughout the 100ns simulation, indicating structural stability for both systems. For RMSF, both peaks were almost overlapping, with fluctuations mostly below 1nm except for a spike near residue 450. 1-Eicosene binding appears to have a very minimal effect on the flexibility of the receptor. For MAO-A, the drug-bound structure displayed a sharp increase in RMSD early period of the simulation (~0.8 nm), suggesting structural deviation or instability, whereas the Phytane-bound system showed a lower and stable RMSD of approximately 0.4–0.5 nm, indicating ligand-induced stabilisation. The RMSF graph indicates that control has more prominent peaks (higher fluctuations), especially toward the C-terminal, compared to the phytochemical, indicating the binding of the phytochemical is more stable. For MAO-B, both the control and phytochemical-bound complexes have stable RMSD trajectories, with the ligand system slightly higher (~0.4–0.5nm) than the control (~0.3–0.4nm), possibly due to conformational adaptation to the ligand. In RMSF, minimal difference was observed for the ligand and control, with slightly elevated values at the terminal residues, which is quite obvious in flexible loop regions.

From the MMPBSA analysis, GGAS value for the $GABA_BR$-1-Eicosene complex was found to be modestly favourable (negative), driven mainly by van der Waals, where GSOLV is slightly unfavourable (positive), largely due to the EPB component. The total binding energy was found to be favourable (-10.03 ± 1.83), indicating stable ligand interaction. In the case of the MAO-A-Phytane complex, the total energy was observed as -26.04 ± 1.94 with favourable GGAS, especially due to van der Waals interactions. GSOLV was observed as moderately unfavourable, but not enough to offset GGAS. Similar to MAO-A, the Total energy for the MAO-B-Phytane complex was highly favourable (-25.6 ± 1.5), suggesting a strong affinity between ligand and protein.

The findings from the *in silico* analysis are well-aligned with the outcomes of the *in-vivo* experiments, collectively supporting the antidepressant potential of *N. jatamansi*. The observed molecular interactions suggest that specific phytochemicals in the plant may exert regulatory effects on dysregulated receptors implicated in depression, underscoring their therapeutic relevance. Several of these phytoconstituents exhibited strong binding affinities toward key neurochemical targets involved in central nervous system function and the pathophysiology of neurological disorders, particularly depression. These results not only provide mechanistic insights but also offer scientific validation for the traditional use of *N. jatamansi* as a neuroprotective agent in the management of CNS-related conditions, including mood disorders. However, the current study

is limited by the lack of pharmacokinetic and toxicity data, as well as the absence of *in vitro* validation of the predicted molecular mechanisms. Future studies addressing these aspects are essential to further substantiate the therapeutic promise of *N. jatamansi*.

5. Conclusion

The present study demonstrates the antidepressant potential of *N. jatamansi* ethanolic extract against electron beam radiation-induced depression, supported by both *in-vivo* and *in silico* analyses. Phytochemicals from *N. jatamansi* showed strong binding affinities to key neurochemical targets, providing mechanistic support for its traditional use as a neuroprotective and antidepressant agent. While these findings are promising, further studies are needed to confirm clinical relevance, including pharmacokinetic, pharmacodynamic, and toxicity assessments, as well as investigations into possible synergistic effects among the phytochemicals.

6. Author Contributions

Conceptualisation - A.G.N. and D.B.; Methodology - A.G.N., S.M. and D.B.; Validation - R.R; Investigation - A.M. and D.B.; Resources - S.M., D.B. and R.R.; Data Curation - A.M.; Writing—original draft preparation - D.B.; Writing, review and editing - A.G.N. and D.B.; Visualisation and and supervision - A.G.N. All the authors have read and agreed to the published version of the manuscript.

7. References

1. Koka K, Verma A, Dwarakanath BS, Papineni RV. Technological advancements in external beam radiation therapy (EBRT): An indispensable tool for cancer treatment. Cancer Manag Res. 2022; 14:1421-1429. https://doi.org/10.2147/CMAR.S351744 PMid:35431581 PMCid:PMC9012312
2. Semwal MK. Khan's the physics of radiation therapy. J Med Phys. 2020; 45(2):134-135. https://doi.org/10.4103/jmp.JMP_17_20 PMCid:PMC7416864.
3. Gao J, Li X, Chen T, Zhao Y, Xiong H, Han X. Application progress of electron beam radiation in adsorption functional materials preparation. Molecules. 2025; 30(5):1084. https://doi.org/10.3390/molecules30051084 PMid:40076308 PMCid:PMC11901924.
4. Li C, Zhang R, Sogore T, Feng J, Liao X, Wang X, *et al.* Electron beam irradiation in food processing: Current applications and strategies for commercial-scale implementation. Sustain Food Technol. 2025; 3(4):875-893. https://doi.org/10.1039/D5FB00006H
5. Banda D, Sucheta K, Rao S. Antidepressant activity of *Nardostachys jatamansi* in electron beam irradiated mice. Int J Res Ayurveda Pharm. 2013; 4(1):101-103. https://doi.org/10.7897/2277-4343.04135
6. Pandey MM, Katara A, Pandey G, Rastogi S, Rawat AKS. An important Indian traditional drug of Ayurveda, *Jatamansi* and its substitute *Bhootkeshi*: Chemical profiling and antioxidant activity. Evid Based Complement Alternat Med. 2013; 2:1-5. https://doi.org/10.1155/2013/142517 PMid:23573115 PMCid:PMC3618914.
7. Mude S, Gulhane S, Mude G, Pise S, Khandar AS. A review on *Nardostachys jatamansi* DC, a flowering plant with therapeutic and pharmacognostic profiles. J Pharmacogn Phytochem. 2020; 870(4):870-873.
8. Thakur S, Kaurav H, Chaudhary G. *Nardostachys jatamansi*: Importance of a highly significant and endangered plant in Ayurveda. Int J Res Ayurveda Pharm. 2021; 12(3):124-130. https://doi.org/10.7897/2277-4343.120387
9. Mane JM, Jagtap JS, Chitlange SS, Nagore DH. Nardostachys jatamansi: A review on extraction, isolation, bioactivities of phytoconstituents, chemical structures and traditional uses. Int J Pharm Qual Assur. 2024; 15(1):475-484. https://doi.org/10.25258/ijpqa.15.1.73
10. Hess B, Kutzner C, van der Spoel D, Lindahl E. GROMACS 4: Algorithms for highly efficient, load-balanced, and scalable molecular simulation. J Chem Theory Comput. 2008; 4(3):435-447. https://doi.org/10.1021/ct700301q PMid:26620784.
11. Valdés-Tresanco MS, Valdés-Tresanco ME, Valiente PA, Moreno E. gmx_MMPBSA: A new tool to perform end-state free energy calculations with GROMACS. J Chem Theory Comput. 2021; 17(10):6281-6291. https://doi.org/10.1021/acs.jctc.1c00645 PMid:34586825.
12. Cryan JF, Slattery DA. GABAB Receptors and depression: Current status. Adv Pharmacol. 2010; 58:427-451. https://doi.org/10.1016/S1054-3589(10)58016-5 PMid:20655491.
13. Anisman H, Merali Z, Poulte MO. Gamma-Aminobutyric Acid Involvement in Depressive Illness Interactions with Corticotropin-Releasing Hormone and Serotonin. The Neurobiological Basis of Suicide. 2012. PMID: 23035295 https://doi.org/10.1201/b12215-5
14. Takahashi A, Shimamoto A, Boyson CO, DeBold JF, Miczek KA. GABA B Receptor modulation of serotonin neurons in the dorsal raphé nucleus and escalation of aggression in mice. J Neurosci. 2010; 30(35):11771-11780. https://doi.org/10.1523/JNEUROSCI.1814-10.2010 PMid:20810897 PMCid:PMC2943331.
15. Ghose S, Winter MK, McCarson KE, Tamminga CA, Enna SJ. The GABA B receptor as a target for antidepressant drug action. Br J Pharmacol. 2011; 162(1):1-17. https://

doi.org/10.1111/j.1476-5381.2010.01004.x PMid:20735410 PMCid:PMC3012402.
16. Liwinski T, Lang UE, Brühl AB, Schneider E. Exploring the therapeutic potential of gamma-aminobutyric acid in stress and depressive disorders through the gut-brain axis. Biomedicines. 2023; 11(12):3128. https://doi.org/10.3390/biomedicines11123128 PMid:38137351 PMCid:PMC10741010.
17. Thompson SM. Modulators of GABAA receptor-mediated inhibition in the treatment of neuropsychiatric disorders: past, present, and future. Neuropsychopharmacol. 2024; 49(1):83-95. https://doi.org/10.1038/s41386-023-01728-8 PMid:37709943 PMCid:PMC10700661.
18. Evenseth LSM, Ocello R, Gabrielsen M, Masetti M, Recanatini M, Sylte I, *et al*. Exploring conformational dynamics of the extracellular venus flytrap domain of the GABA B receptor: A path-metadynamics Study J Chem Inf Model. 2020; 60(4):2294-2303. https://doi.org/10.1021/acs.jcim.0c00163 PMid:32233432 PMCid:PMC7997371.
19. Behl T, Kaur D, Sehgal A, Singh S, Sharma N, Zengin G, *et al*. Role of monoamine oxidase activity in alzheimer's disease: An insight into the therapeutic potential of inhibitors. Molecules. 2021; 26(12):3724. https://doi.org/10.3390/molecules26123724 PMid:34207264 PMCid:PMC8234097.
20. Alsaad I, Abdel Rahman DMA, Al-Tamimi O, Alhaj SA, Sabbah DA, Hajjo R, *et al*. Targeting MAO-B with small-molecule inhibitors: A decade of advances in anticancer research. Molecules. 2024; 30(1):126. https://doi.org/10.3390/molecules30010126 PMid:39795182 PMCid:PMC11722196.
21. Jones DN, Raghanti MA. The role of monoamine oxidase enzymes in the pathophysiology of neurological disorders. J Chem Neuroanat. 2021; 114:101957. https://doi.org/10.1016/j.jchemneu.2021.101957 PMid:33836221.
22. Ostadkarampour M, Putnins EE. Monoamine Oxidase Inhibitors: A review of their anti-inflammatory therapeutic potential and mechanisms of action. Front Pharmacol. 2021; 12. https://doi.org/10.3389/fphar.2021.676239 PMid:33995107 PMCid:PMC8120032.